International Journal of Geosynthetics and Ground Engineering (2025) 11:64
https://doi.org/10.1007/s40891-025-00670-7

TECHNICAL NOTE

Experimental and Analytical Evaluation of Elastic Modulus and MIF in geocell-reinforced Granular Layers Using Benkelman Beam Tests

J. O. Avesani Neto[1] · M. P. Albuquerque[1] · M. C. I. Pérez[2] · J. G. Zornberg[3]

Received: 14 May 2025 / Accepted: 19 October 2025

Abstract

This study presents back-analyses from full-scale road test sections constructed using unreinforced and geocell-reinforced layers and subjected to in-situ deflection tests. The field-testing program was conducted on a 40-m-long test track during the construction of an access road in an industrial facility. An unbound aggregate was adopted for the construction of the subbase and base layers of the pavement structure, with some sections reinforced using two different types of geocell. The field-testing program included a total of 270 Benkelman Beam Tests (BBT), conducted in each of the layers of five different test sections. The test results were used to back-calculate the elastic moduli of the unreinforced and reinforced layers in the different test sections. This allowed for determining the Modulus Improvement Factor (MIF) corresponding to the geocell reinforcements, as well as situating the experimental results within a broader set of literature data to evaluate the accuracy and applicability of an analytical methodology for predicting MIF. The results showed a significant improvement in the elastic modulus of the aggregate layers when using geocell reinforcement, with MIF values ranging from 2.1 to 2.5 depending on the geocell pocket size. The analytical method was found to adequately predict the MIF values, confirming its potential applicability in the design of pavement layers reinforced with geocells.

Keywords Geosynthetics · Pavement reinforcement · Modulus improvement factor · Deflection test · Layered Elastic Theory (LET)

Introduction

Geocells are geosynthetic products with a three-dimensional honeycomb-like pattern of cells, which have been used in several civil engineering areas, such as reinforcement of transportation infrastructure, bearing capacity of shallow foundations, retaining walls, protection of buried pipes, and erosion in slopes and water channels [1–5]. In transportation applications involving unbound granular materials subjected to compaction, both field and laboratory studies have consistently shown that geocell-reinforced layers exhibit increased stiffness [4, 6–9]. The main benefit observed in unbound granular materials stiffening is the high confinement generated during and after the compaction process due to the geocell's capacity to keep the induced horizontal stresses as a prestressed concrete mat [10].

The Modulus Improvement Factor (MIF), defined as the ratio between the moduli of geocell-reinforced and unreinforced layers (Eq. 1), can be used to quantify the improvement due to the presence of a geocell. Typically reported MIF values range from 2.0 to 5.0 based on laboratory

✉ J. O. Avesani Neto
avesani@usp.br

M. P. Albuquerque
michelle.albuquerque@usp.br

M. C. I. Pérez
carolina.ibanez@orbia.com

J. G. Zornberg
zornberg@mail.utexas.edu

[1] Department of Structural and Geotechnical Engineering, Escola Politécnica at the Universidade de São Paulo (EP-USP), travessa 2 nº 83, LMS, São Paulo 05508-010, SP, Brazil

[2] Wavin Geosynthetics, Bogotá, DC, Colombia

[3] Department of Civil, Architectural and Environmental Engineering, The University of Texas at Austin, Austin, TX, USA

Published online: 07 November 2025

experiments, full-scale tests and back-analysis from works [4, 7, 9, 11, 12]. Because geocell-stiffened granular layers can achieve high elastic moduli, their use can lead to significant improvements in pavement performance, such as extended service life or reduced aggregate layer thickness [13]. With the evolution of the Mechanistic-Empirical Pavement Design Guide (MEPDG), a promising approach for quantifying the benefits of geocell reinforcement is through the estimation of the MIF. This parameter enables the direct incorporation of the composite elastic modulus into pavement design calculations (Eq. 1).

$$MIF = \frac{E_{ref}}{E_{un}} \rightarrow E_{ref} = MIF \cdot E_{un} \quad (1)$$

Although some studies have examined the performance of geocell-reinforced aggregate materials in pavement applications, data on their behavior during both construction and service life in real-world projects remain limited. Establishing a comprehensive database that captures construction and post-construction performance under field conditions is a crucial step toward the broader acceptance and implementation of innovative technologies such as geocell-stiffened aggregates.

To contribute to the state of the practice for full-scale experiments on geocell system performance, this study presents the back-analysis of deflection results from Benkelman Beam Tests (BBT) conducted on several unreinforced and reinforced test sections. A full-scale test program was carried out on roadway test sections to evaluate the MIF generated by different geocells in a typical aggregate material layer used in pavement structures under field conditions. The test sections, involved two- and three-layer systems in unreinforced and reinforced conditions, were back-analyzed to obtain the elastic modulus using a Layered Elastic Theory (LET) -based software. Comparisons were also conducted involving the results of several field tests conducted on pavement structures as well as the outcomes of an MIF analytical method.

Table 1 Summary of soil properties

Parameter	Subgrade soil	GSB aggregate material
Unit weight, γ (kN/m^3)	14.6	23.2
Fines fraction (%)	90	16
Water content, w (%)	29	6.9
Liquid Limit, LL	51	21
Plastic Limit, PL	24	11
Plasticity Index, PI	27	10
USCS classification	CH-CL	GC
HRB classification	A-7-6 (18)	A-2–4
Undrained shear strength, S_u (kPa)	3.8 to 12.0	-
Friction angle, φ (°)	-	38
California Bearing Ratio, CBR (%)	1.2 to 4.2	23

Materials and methods

Materials

The natural in-situ material at the field test site was used as subgrade of the test sections. It can be characterized as a soft silty clay with 90% fines (fraction smaller than the 75-µm sieve), a specific gravity of solids (G_s) of 2.48, a Liquid Limit (LL) of 51 and a Plasticity Index (PI) of 27. The in-situ water content and unit weight at the time of construction of the test sections were determined as 29% and 14.6 kN/m³, respectively. The subgrade was classified as a clay with low to high plasticity (CH-CL) according to the Unified Soil Classification System (USCS), and as A-7-6 according to the AASTHO classification system. Before test section construction, California Bearing Ratio (CBR) tests were conducted on the subgrade, which were found to range from 1.2% to 4.2%. In addition, mini vane shear tests were carried out on the subgrade, also prior to construction and, which resulted in undrained shear strength (S_u) values ranging from 3.8 to 12 kPa. Table 1 presents a summary of the subgrade properties.

The aggregate material for the unreinforced and reinforced top layers consisted of a typical Granular Subbase (GSB) material. The GSB had a fines fraction of 16%, a G_s of 2.6, and LL and PI of 21 and 10, respectively. The maximum dry unit weight (γ_{dmax}), obtained from a Modified Proctor Compaction (MPC) test, was 21.7 kN/m^3 for an optimum water content (w_{opt}) of 6.9%. The friction angle (φ), obtained from direct shear, and CBR were 38° and 23%, respectively, as obtained for samples prepared at the 100% of the maximum relative compaction according to the Modified Proctor Compaction test. The GSB was classified as clayey gravel (GC) and A-2–4 according to the USCS and AASTHO systems, respectively. Table 1 provides a summary of the GSB aggregate characteristics.

Two types of High-Density Polyethylene (HDPE) geocells manufactured by Wavin Geosynthetics were used in this study. Geocell A was characterized by a height of 150 mm and a weld spacing of 345 mm (when the cell was folded), which correspond to a pocket cell area of 0.048 m² and an equivalent diameter of 247 mm. Geocell B was characterized by a height, weld spacing, pocket cell area, and equivalent diameter of 120 mm, 445 mm, 0.029 m² and 193 mm, respectively. The geocell walls were textured and perforated. The wall thickness was 1.5 mm thick, with an elastic modulus equal to 700 MPa [14]. A summary of the geocell characteristics is provided in Table 2.

Table 2 Summary of geocell characteristics (Wavin Geosynthetics, 2023)

Parameters	Geocell A	Geocell B
Polymer	HDPE	HDPE
Weld spacing (mm)	445 mm	356 mm
Open cell dimensions (mm)	315 − 304	259 − 226
Cell open area (m^2)	0.048	0.029
Equivalent diameter (mm)	247	193
Cell wall height (mm)	150	120
Cell wall thickness (mm)	1.5	1.5
Elastic modulus (MPa)	700	700
Geocell wall stiffness (kN/m)	1050	1050

Details and Construction of the Test Sections

A total of five full-scale field Test Sections were constructed as part of the construction of an access road to an industrial facility located in Bogotá, Colombia. The overall experimental track of the access road was 40 m in length and 3.5 m in width and included five 8-m-long Test Sections constructed with different combinations of unreinforced and geocell-reinforced granular layers. Benkelman Beam Test (BBT) for deflection measurement, typically adopted for construction quality control, were conducted in each layer of the different Test Sections. For each 8 m Test Section, the BBT was carried out by positioning the beam and vehicle along the section and performing the standard vehicle movement required for the measurements.

BBT is a straightforward and cost-effective deflection-based method commonly used for quality control across all pavement layers in various transportation infrastructure projects. The BBT deflection method is also recommended for conducting quality control and evaluating the benefits of geocell-reinforced pavement structure layers [15]. During testing, the Benkelman beam is positioned between the dual tires of a Simple Axle Dual Tire vehicle, which applies an 80 kN load at a tire pressure of 560 kPa, producing two equivalent circular loads spaced 288 mm apart. Deflection criteria for each pavement layer are defined based on the road's functional requirements and design life, and the BBT is used to evaluate compliance with these criteria. The procedures followed in this study were in accordance with U.S. standards [16].

All Test Sections were constructed using the same GSB aggregate material and a total thickness (H) of 400 mm, but they differed on the type and location of the geocell reinforcement, with geocell reinforcement adopted for the subbase and/or base layers. The different configurations adopted for the different Test Sections aimed at facilitating the comparison of modulus improvements resulting from the presence of a geocell reinforcement.

Figure 1 presents cross-sections of the five Test Sections evaluated in this study. As indicated in this Figure, Test Sect. 1 was the Control Section, with the GSB unreinforced subbase and base layers measuring 150 mm and 250 mm in thickness (H), respectively. Test Sect. 2 involved GSB subbase and base layers, both of which were 200 mm thick (H), reinforced with Geocell A, herein referred to as GSB_{gA} (where 'gA' denotes a Geocell A-reinforced layer). Test Sect. 3 had a 200-mm-thick unreinforced subbase layer directly over the subgrade, and a 200-mm-thick GSB_{gA} base layer over the unreinforced subbase layer. Test Sect. 4 had a 200-mm-thick GSB_{gA} subbase layer under a 200-mm-thick unreinforced base layer. Finally, Test Sect. 5 was constructed with a 150-mm-thick GSB_{gB} subbase layer (where 'gB' denotes a Geocell B-reinforced layer) under a 250-mm-thick unreinforced base layer.

Figure 2 illustrates the construction steps, which were similar across all Test Sections. These included subgrade compaction and base layer preparation (Fig. 2A), placement of the layers with or without reinforcement (Fig. 2B), compaction of each layer (Fig. 2C) and performance of the BBT (Fig. 2D). All GSB layers were compacted using a single smooth-drum vibratory roller, with a width of 2.0 m and centrifugal roller drum force equal to 150 kN, with a target of 100% of the maximum relative compaction according to the Modified Proctor Compaction test.

Table 3 provides details on the BBTs conducted on the different layers of the five Test Sections, named as Test Series, in addition to a complementary summary of the variables considered in the full-scale test program, including BBT deflection results, back-calculated elastic moduli, and the MIF for each Test Section, which will be analyzed in detail in Sect. 3. As shown in Table 3, Test Series A refers to the BBTs performed directly on the subgrade across all five Test Sections. Test Series B, B_{gA}, and B_{gB} correspond to BBTs conducted on the subbase layer after its installation and compaction, either without or with geocell reinforcement. Specifically, Test Series B represents the unreinforced subbase, while B_{gA} and B_{gB} refer to subbases reinforced with Geocell A and Geocell B, respectively. Lastly, Test Series C and C_{gA} denote BBTs carried out on the base layer after compaction, without and with Geocell A reinforcement, respectively. A total of 54 BBT deflection measurements − 18 on each of the subgrade, subbase, and base layers - were recorded for each Test Section, resulting in 270 deflection measurements across the entire full-scale field test track.

Results and Discussion

Table 3 presents the BBT average deflection and Coefficients of Variation (COV) obtained for each Test Series. The average deflections obtained from the BBT testing program

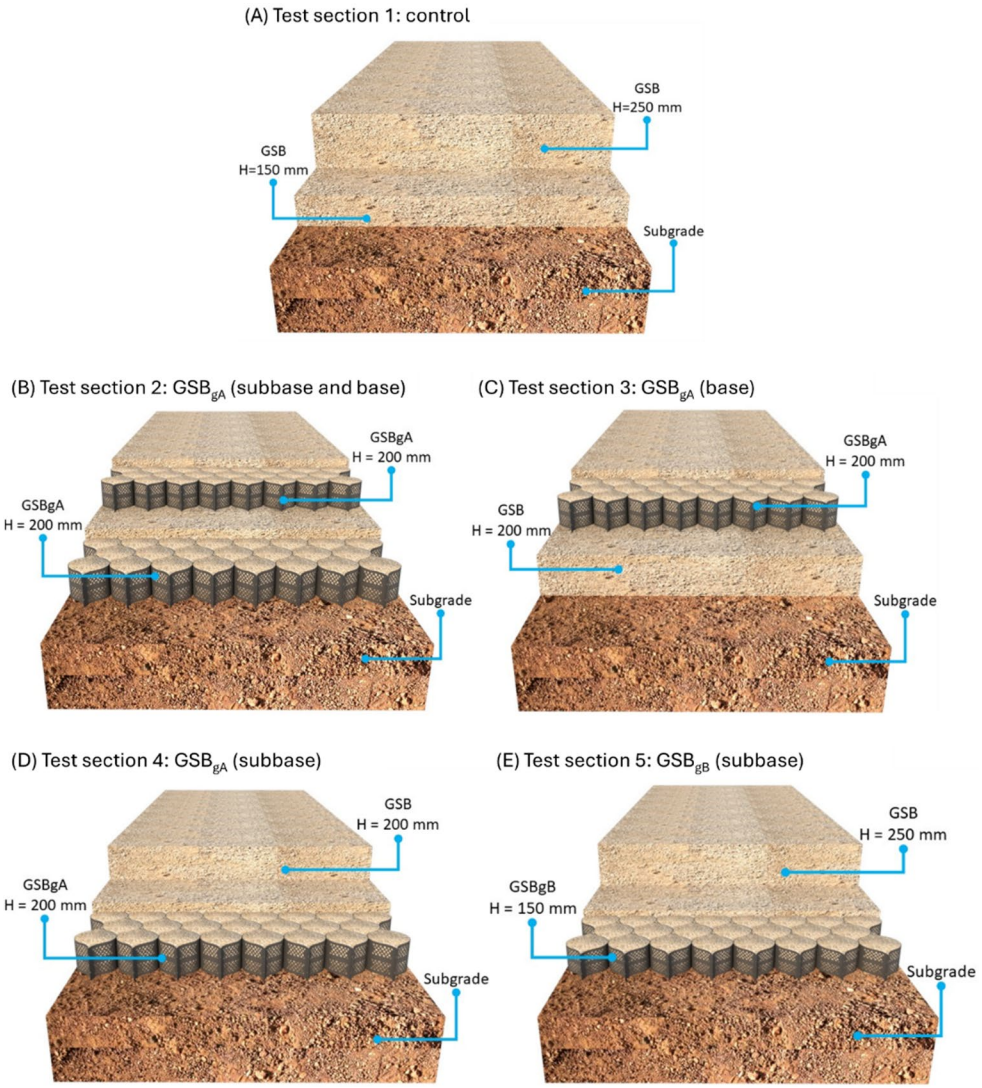

Fig. 1 Schematic illustration of full-scale field test conducted: (**A**) Test Sect. 1: control (unreinforced subbase and base); (**B**) Test Sect. 2: Geocell A-reinforced subbase and base; (**C**) Test Sect. 3: unreinforced subbase and Geocell A-reinforced base; (**D**) Test Sect. 4: Geocell A-reinforced subbase and unreinforced base; (**E**) Test Sect. 5: Geocell B-reinforced subbase and unreinforced base

range from 1.46 to 4.31 mm, with the COV ranging from 15% to 38%. Comparatively higher average deflections and COV were obtained from tests conducted on the subgrade surface (i.e., Test Series A). These trends are consistent with the comparatively low modulus expected in subgrade soils, as well as their comparatively high heterogeneity in relation to the other roadway layers. For the BBTs conducted over the subbase and base layers, both the average deflection and COV values were found to decrease. The decrease in average deflections was more significant in BBTs conducted on base layers (i.e., Test Series C and C_{gA}), possibly due to comparatively thicker pavement structure over the subgrade. The COV values were comparatively smaller for the BBTs conducted over the base layer (Test Series C and C_{gA}) and reinforced subbase layer in Test Series B_{gA} - almost 40% smaller than the COV resulting from BBTs conducted on the subgrade.

Inspection of the average deflection values in Table 3 indicates that the results obtained in geocell-reinforced layers were not significantly smaller than those obtained in unreinforced layers. However, except for Test Series B_{gB}, the average deflections shown in Table 3 correspond to values obtained using results from more than one Test Section. As the deflection of subbase and base is influenced by the subgrade deformability, the deflection results in Table 3 do not capture the full improvement attributable to the geocell. This limitation highlights the fact that deflection measurements alone provide a global response of the pavement system, in which the subgrade deformability can overshadow the contribution of the reinforced layers. The back-analysis using the Layered Elastic Theory (LET) allows isolating the deformability of each layer, thereby quantifying the reinforcement effect more clearly. In this sense, although the average deflections in reinforced layers were not always lower than in the unreinforced condition,

Fig. 2 Test Sections construction: **A**) base layer preparation; **B**) filling of geocell-reinforced layer; **C**) compaction operations; and **D**) deflection test (BBT) being conducted on one of the constructed layers

Table 3 Summary of characteristics and results for the different test series

Test Series	Layer	Material	Test Sections	Average Deflection (mm)	COV	E_{un} (MPa)	E_{ref} (MPa)	MIF experimentally obtained	MIF analytically predicted[1]
A	Subgrade	Subgrade	1 to 5	4.31	38%	18	-	-	-
B	Subbase	GSB	1 and 3	2,0.30	32%	212	-	-	-
C	Base	GSB	1, 4 and 5	1.69	15%		-	-	-
B_{gA}	Subbase	GSB_{gA}	2 and 4	2.20	18%	-	443	2.09	2.38
C_{gA}	Base	GSB_{gA}	2 and 3	1.46	15%	-			
B_{gB}	Subbase	GSB_{gB}	5	3.29	33%	-	540	2.54	2.59

[1] Predicted using the analytical MIF methodology by Garcia and Avesani Neto (2021)

the higher back-calculated moduli of the reinforced layers confirm the improvement provided by the geocell reinforcement, with the larger surface deflections primarily reflecting the influence of the subgrade. The next section explores this evaluation.

Layer Elastic Modulus (E) back-analysis

ELLEA1, an LET-based software, was used to back-analyze the BBT results in each layer [17]. This software has previously been used to analyze road pavement structures, including those with geosynthetic reinforcements, including geocells [4, 18]. The methodology adopted in this investigation is consistent with that followed in previous studies, whereby the BBT results were employed in an iterative process [4, 6, 12]. The input parameters included each layer thickness and Poisson's ratio, as well as the sizing and magnitude of the load applied during the BBT, resulting in a predicted vertical deflection.

Each layer's thickness (H) in the analyses corresponds to that in the experimental full-scale field test and is presented in Fig. 1. The applied load geometry and load magnitude followed the BBT standards. The adopted Poisson's ratios (ν) were 0.45, 0.35, and 0.25 for the subgrade, unreinforced GSB, and geocell-reinforced GSB, respectively, based on values reported in guidelines and previous studies [4, 9, 12, 19].

The layer elastic moduli values, for unreinforced (E_{un}) and reinforced (E_{ref}) situations, obtained from the back-calculation based on the LET analysis are presented in Table 3. These moduli were calculated using the BBT average deflection results from the Test Sections for each Test Series, as shown in the table. It should be noted that average surface deflections do not directly translate into moduli layers, as they reflect the combined deformability of all pavement layers. The LET back-analysis isolates each layer's contribution, providing consistent elastic modulus values even when surface deflections vary. The layer moduli were obtained through an iterative process in which each layer's moduli ware adjusted until the calculated deflections matched the average BBT measurements for the corresponding Test Section.

As observed in Table 3, considering the average deflection obtained in Test Series A with the BBT conducted directly over the subgrade in Test Sects. 1 to 5, the back-analyzed elastic modulus was equal to 18 MPa. The subgrade elastic modulus was found to range from 11 to 31 MPa in Test Sects. 1 to 5, showing good agreement with several correlations with the CBR [20, 21].

As also shown in Table 3, the unreinforced elastic modulus (E_{un}) obtained for the unreinforced GSB material is 212 MPa, calculated as the average of the back-calculated moduli from Test Series B and C in Test Sects. 1, 3, 4, and 5. The reported modulus represents the averaged response across the Test Sections, acknowledging natural variability in the material properties and test execution. This value falls within the range of 200 to 300 MPa recommended by several studies and transportation agencies for typical GSB layers classified as GP-GW according to the USCS [19, 22]. However, the GSB material used in this study is classified as GC under the USCS, and therefore, a slightly lower elastic modulus is expected in comparison to GP-GW materials due to its higher fines content and cohesive behavior.

The inclusion of geocell reinforcement in the GSB aggregate material resulted in a significant increase in the elastic modulus of the layer, as evidenced by the back-calculated moduli (E_{ref}) presented in Table 3. The moduli for the geocell-reinforced layers, in Test Series B_{gA}, C_{gA}, and B_{gB}, were 443 MPa and 540 MPa for the layers reinforced with Geocell A (GSB_{gA}) and Geocell B (GSB_{gB}), respectively. These values are substantially higher than those of the unreinforced condition (E_{un}), representing increases of approximately 110% to 150%. This improvement is primarily attributed to the enhanced confinement provided by the geocell reinforcement. Since GSB aggregate is an unbound granular material sensitive to the stress state, increased confinement leads to greater shear strength and stiffness, particularly when compaction is effectively performed. A comparison between the moduli of reinforced and

unreinforced layers will be used to determine the MIF in the next section.

Modulus Improvement Factor (MIF) Evaluation

MIF is a relevant parameter that quantifies the improvement achieved by the inclusion of geocells in a pavement layer. Its use is particularly helpful to facilitate the design of roadways involving geocell-reinforced layers because it allows for direct incorporation of the elastic modulus of reinforced layers. In MEPDG analyses, the modulus of the geocell-reinforced layer can be predicted if the MIF and the unreinforced elastic modulus are known (Eq. 1).

The BBT full-scale test results in Test Series B_{gA}, C_{gA} and B_{gB} allowed determination of the MIF values corresponding to both Geocell A (GSB_{gA}) and Geocell B (GSB_{gB}), and are presented in Table 3. The MIF values were obtained as the ratio between the E_{ref} (for both geocells) and E_{un}.

The results in Table 3 show that the MIF obtained using the geocell ranged between 2.09 and 2.54. The Geocell A-reinforced GSB aggregate (Test Series B_{gA} and C_{gA}) resulted in an MIF of 2.09 and the Geocell B-reinforced GSB aggregate (Test Series B_{gB}) resulted in an MIF of 2.54. The MIF results obtained in this study are consistent with the values reported in the literature.

As indicated by the results shown in Table 3, the MIF value obtained for Geocell B is comparatively higher than that obtained for Geocell (A) This trend can be attributed to the relative stiffness index, S_i, found in Eq. 2, which is the most influential parameter for obtaining and in direct proportionality to the MIF [10]. The S_i is influenced by the geocell pocket size, which is represented in Eq. 2 by the equivalent diameter (d_{eq}) of the open, filled cell. A smaller d_{eq} leads to a higher S_i value, and consequently, a higher MIF. Since Geocell B has a d_{eq} approximately 80% smaller than that of Geocell A, a greater MIF is expected for Geocell (B) This expectation aligns with the trend observed in the experimental test results.

$$S_i = \frac{2J}{kP_a d_{eq}} \tag{2}$$

where J is the geocell wall stiffness; k the soil modulus number in the hyperbolic constitutive soil model [23]; P_a the atmospheric pressure; and d_{eq} the equivalent cell diameter.

Table 3 also presents the theoretical MIF value estimated using the analytical methodology proposed by Garcia and Avesani Neto (2021). To predict the MIF using this analytical method, GSB aggregate hyperbolic parameters were adopted based on recommended parameters reported in the literature for similar materials [23, 24] as: $\gamma = 21.7$ kN/m^3; $c' = 0$; $\varphi' = 38°$; $R_f = 0.8$; $k = 600$; $k_u/k = 1.2$; and $n = 0.4$ – where k_u, n and R_f are the modulus number for unloading, modulus exponent, and failure ratio, respectively, of the hyperbolic constitutive soil model. The geocell characteristics presented in Table 3 were used. The stress generated by the compaction process was estimated using an analytical method [24] considering the previously mentioned procedures and equipment used during construction.

Using the MIF analytical method, MIF values of 2.38 and 2.59 were obtained for Geocells A and B, respectively, as also provided in Table 3. The analytical predicted MIF values are similar to those experimentally obtained using the deflections and elastic moduli from the experimental full-scale field tests. For Geocell A (Test Series B_{gA} and C_{gA}), the absolute and relative differences between the MIF experimentally obtained and the analytically predicted were 0.29 and 14%, respectively. For Geocell B (Test Series B_{gB}), the same absolute and relative differences were 0.05 and 2%, respectively.

Figure 3 compares the experimentally obtained MIF values with the analytically predicted ones for the experimental full-scale field test presented herein. The results from experimentally obtained and analytically predicted MIF results from previous studies [4, 10, 12] are also presented in Fig. 3.

The good agreement between the MIF values predicted using the analytical method and those obtained from experiments can be verified by the results presented in Fig. 3. Considering the significant variability of experimental conditions captured by the several points in this Figure, such as test type (laboratory, full-scale in the field and back-analyzed works), applied load (static and cyclic PLT, BBT and FWD), geocell reinforcement characteristics (several raw materials, cell thickness, height and pocket size), fill soil (several types of sand, crushed rock and coarse materials) and compaction conditions, the analytical method is found to satisfactorily estimated the MIF. In particular, the predictions were compared against a comprehensive set of 30 literature points covering a wide range of geocell types, aggregates, subgrade conditions, loading modes, and experimental settings, demonstrating robust predictive capability across diverse scenarios. The use of the MIF analytical methodology may provide a practical means to estimate the modulus of specific layers during preliminary analyses in projects involving geocell-reinforcement applications.

Limitations

The experimental results presented in this study are specific to the subgrade, climate, and traffic conditions of the tested site. The BBTs were conducted immediately after compaction of each pavement layer, reflecting only the initial stiffness improvements. Unlike repeated load experiments such as FWD or cyclic plate load tests, the BBT directly simulates

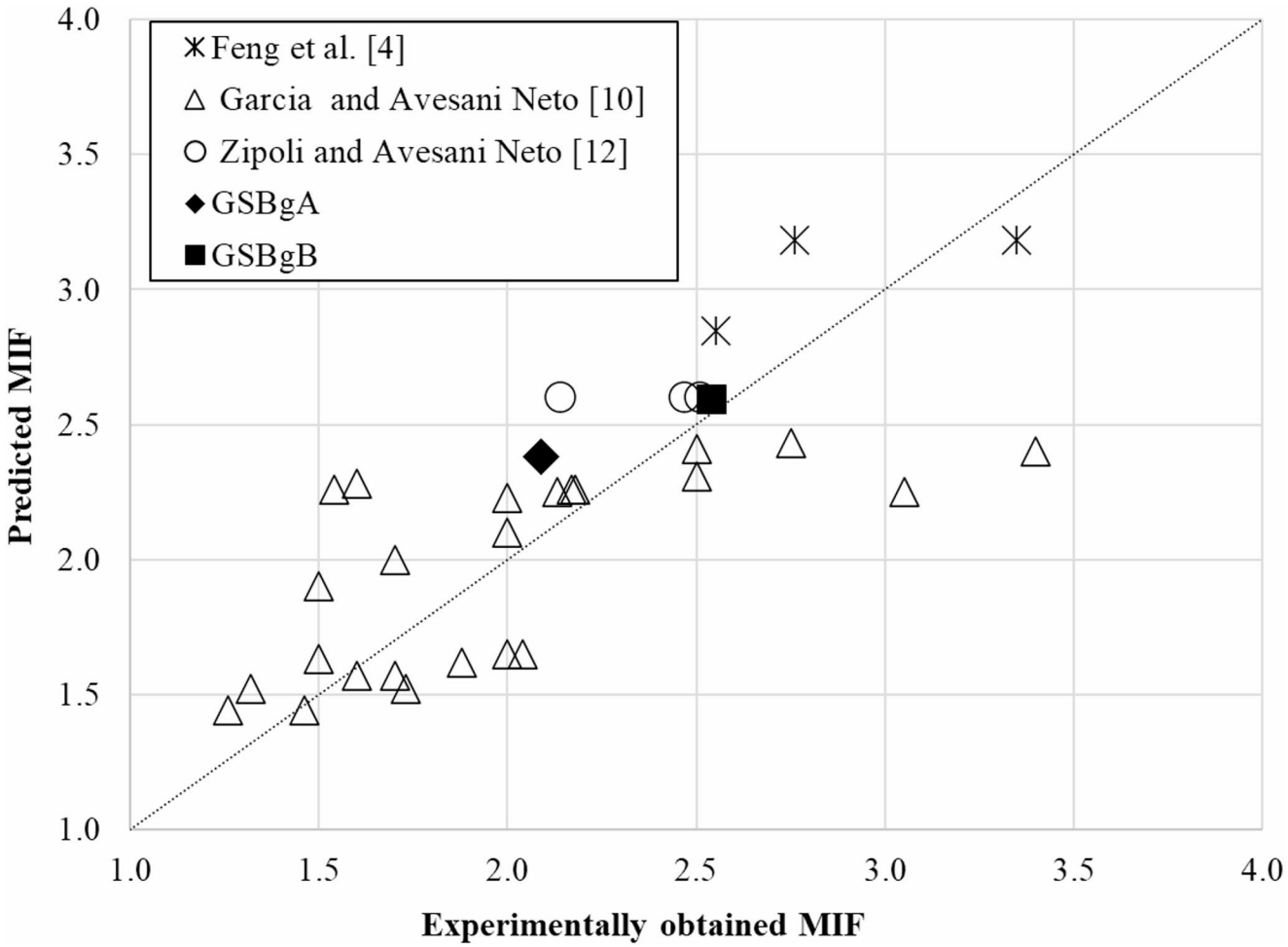

Fig. 3 Comparison between MIF values obtained experimentally in several studies and predicted via MIF analytical method

standard axle loading conditions, providing realistic insight into pavement response under typical design loads. However, because the BBT is not cyclic, the reported MIF represents short-term values, which may evolve over time due to traffic loading, environmental effects, or material fatigue. Furthermore, the experimental program considered only specific geocell products and a single infill material. The findings should therefore be interpreted with caution when applied to different soil, geocell, or traffic conditions, or for long-term pavement performance, and further validation under diverse scenarios is recommended.

Also, practical implementation factors, including material and installation costs, construction quality, and long-term maintenance, are acknowledged as relevant considerations. However, these aspects were not evaluated in the present study, which focuses exclusively on field-observed mechanical performance, and could be addressed in future investigations.

Conclusions

This study presented back-analyses from full-scale field experiments with unreinforced and geocell-reinforced layers subjected to in situ deflection tests. An unbound granular material comprising a typical Granular Subbase (GSB) aggregate was utilized as the subbase and base layers. Two geocells with different dimensions were employed as reinforcement. Five different Test Sections were constructed over the 40-m-long test track: one unreinforced Test Section for control purposes and four reinforced Test Sections to evaluate the improvement in GSB aggregate attributable to the geocell. Deflection in-situ tests were carried out using the Benkelman Beam Test (BBT) performed on the different pavement soil layers: subgrade, subbase and base. The elastic moduli in the unreinforced and reinforced layers were back-calculated in the different Test Sections using LET-based software. This allowed determination of the Modulus Improvement Factor (MIF) experimentally obtained by the geocell reinforcements, and evaluation of the accuracy

of an analytical method for estimating the MIF. Based on the results of this study, the following conclusions can be drawn:

- The GSB aggregate elastic moduli were significantly improved due to the presence of geocell reinforcement, resulting in MIF values ranging from 2.09 to 2.54 in the full-scale field test.
- Geocell B, with a smaller cell pocket size, generated a 20% higher MIF than Geocell B, which had a larger cell pocket size.
- The MIF value predicted using an analytical methodology (Garcia and Avesani, 2021) showed good agreement with the results from the full-scale field test. A comparison of this full-scale test with other laboratory and field experiments confirmed the significant prediction potential of the MIF analytical approach.
- The BBT proved to be an effective tool for determining the elastic moduli of both unreinforced and geocell-reinforced layers, as well as for evaluating and controlling the MIF during pavement layer construction.

Acknowledgements The authors would like to acknowledge the Wavin Geosynthetics for supporting the experimental program, and the support provided by the São Paulo Research Foundation (FAPESP grant 2023/04447-1) and National Council of Scientific and Technological Development (CNPq grant 305309/2024-2).

Author Contributions J. O. Avesani Neto: Conceptualization, Formal Analysis, Supervision, Validation, Writing – Original Draft. M. P. Albuquerque: Data curation, Investigation, Methodology, Formal Analysis. M. C. I. Pérez: Conceptualization, Resources, Visualization. J. G. Zornberg: Validation, Writing – Review & Editing.

Data Availability Data are available upon request.

Declarations

Conflict of interest The authors declare no conflict of interest.

References

1. Babagiray G, Oguzhan Akbas S, Anil O (2023) Full-scale field impact load experiments on buried pipes in geosynthetic-reinforced soils. Transp Geotech 38:100927. https://doi.org/10.1016/j.trgeo.2022.100927
2. Saikia R, Dash SK (2024) Load carrying mechanism of geocell reinforced embankment on soft soil. Transp Res Rec. https://doi.org/10.1177/03611981241230317
3. Khan MA, Puppala AJ (2023) Sustainable pavement with geocell reinforced reclaimed-asphalt-pavement (RAP) base layer. J Clean Prod. https://doi.org/10.1016/j.jclepro.2022.135802
4. Feng LX, Avesani Neto JO, Zornberg JG (2024) Evaluation of the elastic modulus improvement in geocell-reinforced unbound aggregates: full-scale experimental sections on a highway. Transp Geotech 49:101444. https://doi.org/10.1016/J.TRGEO.2024.101444
5. Rezende JCV, Avesani Neto JO, Zornberg JG (2024) Shear Strength Characterization of the Interface Between Geocell Walls and Infill. Indian Geotechnical Journal 1–12. https://doi.org/10.1007/S40098-024-01108-Z/METRICS
6. Avesani Neto JO (2019) Application of the two-layer system theory to calculate the settlements and vertical stress propagation in soil reinforcement with geocell. Geotext Geomembr 47:32–41. https://doi.org/10.1016/j.geotexmem.2018.09.003
7. Gottumukkala B, Mehar B, Minchala D et al (2023) Laboratory and field evaluations of geocell reinforced bases for locally available material in the Himalayan region. Int J Geosynth Ground Eng. https://doi.org/10.1007/s40891-023-00497-0
8. Banerjee S, Manna B, Shahu JT (2023) Geocell as a promising reinforcement technique for road pavement: a state of the art. Indian Geotech J. https://doi.org/10.1007/s40098-023-00818-0
9. Baby LM, Avesani Neto JO (2024) Evaluation of geocell-reinforced railway track using FEM and FLM-based software: a parametric analysis. Int J Geosynth Ground Eng 10:1–9. https://doi.org/10.1007/S40891-024-00564-0
10. Garcia RS, Avesani Neto JO (2021) Stress-dependent method for calculating the modulus improvement factor in geocell-reinforced soil layers. Geotext Geomembr 49:146–158. https://doi.org/10.1016/j.geotexmem.2020.09.009
11. Inti S, Tandon V (2021) Design of geocell reinforced roads through fragility modeling. Geotext Geomembr 49:1085–1094. https://doi.org/10.1016/J.GEOTEXMEM.2021.03.003
12. Zipoli LLR, Avesani Neto JO (2022) Evaluation of back-calculated elastic moduli of unreinforced and geocell-reinforced unbound granular material from full-scale field tests. Geotext Geomembr 50:910–921. https://doi.org/10.1016/J.GEOTEXMEM.2022.05.006
13. Zornberg JG (2017) Functions and applications of geosynthetics in roadways. Transp Geotechnics Geoecology 189:298–306. https://doi.org/10.1016/j.proeng.2017.05.048
14. Wavin G (2023) Geocells specifications
15. Giroud JP, Han J (2016) Part 2: field evaluation of the performance of unpaved roads incorporating geosynthetics—Planning, vol 34, 2No. edn. Geosynthetics
16. AASHTO T 256 (2016) Standard Method of Test for Pavement Deflection Measurements
17. Levenberg E (2016) ELLEA1: Isotropic Layered Elasticity in Excel: Pavement analysis tool for students and engineers - Excel spreadsheet. In: DTU Library. https://orbit.dtu.dk/en/publications/ellea1-isotropic-layered-elasticity-in-excel-pavement-analysis-to. Accessed 3 Dec 2023
18. Bahrani N, Levenberg E, Blanc J, Hornych P (2020) General Rights Inverse Analysis of Pavement Layer Moduli Based on Data Collected by Buried Accelerometers and Geophones. In: Proceedings of 6th APT Conference. Springer, pp 592–601
19. National Cooperative Highway Research Program. (2004). Guide for mechanistic-empirical design of new and rehabilitated pavement structures: Final report (NCHRP Project 1-37A). Transportation Research Board, National Research Council
20. Powell WD, Potter JF, Mayhew HC, Nunn ME (1984) The structural design of bituminous roads
21. Heukelom W, Klomp A (1962) Dynamic testing as a means of controlling pavements during and after construction. In: International Conference on the Structural Design of Asphalt PavementsUniversity of Michigan, Ann Arbor
22. Yoder EJ, Witczak MW (1975) Principles of pavement design. Wiley-Interscience Publication, John Wiley & Sons, Inc.,, London ? pp
23. Duncan JM, Byrne P, Wong KS, Mabry P (1980) Strength, Stress-strain and Bulk Modulus Parameters for Finite Element Analyses of Stresses and Movements in Soil Masses. California

24. Ehrlich M, Mitchell JK (1994) Working stress design method for reinforced soil walls. J Geotech Eng. 120(4):625–645 https://doi.org/10.1061/(ASCE)0733-9410(1994)120:4(625)